KINETIC STUDY OF Al_2O_3 SINTERING BY DILATOMETRY

ZUZANA HOLKOVÁ, LADISLAV PACH, VLADIMÍR KOVÁR, ŠTEFAN SVETÍK

Department of Ceramics, Glass and Cement, Faculty of Chemical and Food Technology, Slovak University of Technology, Radlinského 9, 812 37 Bratislava, Slovak Republic

E-mail: zholkova@vucht.sk

Submitted September 30, 2002; accepted March 14, 2003

Keywords: Al_2O_3, Boehmite, Sintering, Dilatometry, Ceramic membranes

Sintering of a-Al_2O_3 powder (particles ≈ 1 μm), boehmite gels (particles ≈ 5 nm) and compositions of a-Al_2O_3, boehmite and graphite has been studied by stepwise (SID) and individual (IID) isothermal dilatometry. Boehmite gel is a high temperature binder and graphite is a pore forming material in the mentioned compositions. Boehmite derived alumina controls the sintering process of compositions if it is present as a continuous phase. Kinetic parameters of sintering (exponent n and apparent activation energy E) indicate different sintering mechanism of α-Al_2O_3 and Al_2O_3 derived from boehmite gels. Porosity of α-Al_2O_3 ceramics can be managed by joint addition of boehmite gel and graphite.

INTRODUCTION

Porous ceramics have a wide range of applications including filters, insulators, catalyst supports, separation membranes, etc. [1, 2]. Ceramic membranes are of great interest in separation technology because of their higher chemical, thermal and mechanical stability, compared to organic membranes, tolerance to solvents, as well as to *pH*, oxidation, and temperature extremes, their durability and good defauling properties [3]. An ideal ceramic membrane must be highly selective, permeable and durable [4, 6]. The membrane selectivity primarily depends on the pore size distribution - the narrower is the pores size distribution, the more selective is the membrane.

Many properties of the final ceramics, such as density or porosity, strongly depend on a green body microstructure and on conditions under which the green body is sintered. One of the most important parameters is the temperature program during sintering, especially the heating rate. During the sintering process, microstructural changes occur as a result of a complex interplay of various material transport mechanisms. This necessitates a deeper understanding of the process [6].

Diffusion is accepted as a control mechanism in high temperature sintering of fine-grained materials. The dominant path for diffusion is usually noted along the grain boundary [7]. Grain-boundary diffusion and interface reaction are two sequential processes in diffusion processes. The slower mechanism will dominate the sintering process. The smaller is the mean grain size, the shorter is the transportation path and therefore the faster is the occurred grain-boundary diffusion. Therefore, interface reaction becomes important.

Dilatometry experiments are a well-known way to study the densification kinetics during sintering [8, 9]. Apparent activation energy and the shrinkage rate can be calculated from measured shrinkage dependencies vs. time and temperature.

Ali and Sorenson [10] described an evaluation of the kinetic parameters from the analysis of a stepwise isothermal dilatometry (SID) data for low temperature sintering of TZO ceramics.

Wang et al. [11] applied this technique to evaluate kinetic parameters from SID data obtained during sintering and pore-forming process of macroporous α-Al_2O_3 ceramics prepared by extrusion. Kinetic parameters, i.e., the average exponent *n* (parameter related to the process mechanism) and the apparent activation energy *E* of the pore-forming process, were calculated to be 0.232 and 415.5 kJ/mol, respectively, in the temperature range of 1200 - 1400°C.

Authors of SID method studied the sintering of α-Al_2O_3 powder sized ≈ 16 μm. The aim of this work is to verify the possibility of using this method for significantly finer particles of α-Al_2O_3 (≈ 1μm) and boehmite derived alumina gels (≈ 5 nm). Commercial α-Al_2O_3 powder, PVA and boehmite gel (as binders) and graphite (as pore forming material) were used to prepare porous alumina ceramics potentially applicable for ceramics membranes.

THEORETICAL

Sintering of powder compacts or castings is as a rule accompanied by shrinkage. Its time dependence indicates the nature of individual processes and is recorded as

$$\Delta l/l_0 = f\,(t,\ \tau,\ r) \tag{1}$$

dependency, where $\Delta l/l_0$ is relative shrinkage, t - temperature, τ - time and r - particle radius.

For the mentioned aim of this work, kinetics of isothermal sintering is expressed according to Ali and Sorensen's equation [10] derived for volume shrinkage

$$\frac{V_0 - V_\tau}{V_0 - V_f} = \frac{[k_T(\tau - \tau_{0,T})]^n}{1 + [k_T(\tau - \tau_{0,T})]^n} \tag{2}$$

where V_0 is the initial volume of the green body, V_τ the volume at time τ, V_f the volume of a fully densed sample, τ the sintering time, $\tau_{0,T}$ the formal beginning of isothermal sintering, k_T the specific rate constant, n the parameter related to a sintering mechanism.

The case when cylinder shaped samples are used and isotropic sintering is assumed (d_τ/l_τ = const.; d_τ, and l_τ - diameter and length, resp. of a cylinder in the time τ) gives

$$\frac{V_0 - V_\tau}{V_0 - V_f} = \frac{l_0^3 - l_\tau^3}{l_0^3 - l_f^3} = \frac{[k_T(\tau - \tau_{0,T})]^n}{1 + [k_T(\tau - \tau_{0,T})]^n} \tag{3}$$

and the equation (3) for l_τ yields

$$l_\tau = \sqrt[3]{l_0^3 - (l_0^3 - l_f^3)\frac{[k_T(\tau - \tau_{0,T})]^n}{1 + [k_T(\tau - \tau_{0,T})]^n}} \tag{4}$$

where similarly l_0 is the initial length and l_f the length of a fully densed sample.

The length changes of the samples are observed under dynamic or isothermal conditions of temperature treatment. Mathematical description of the process kinetics is more favorable for isothermal methods then for dynamic ones, but it needs much more experimental data. SID method developed by Meng and Sorensen [12] may be considered as a combined dynamic-isothermal method. It enables to obtain classical process description out of the single experiment. This procedure is based on measuring isothermal dilatometry data of shrinkage z vs. experiment time τ at some temperatures (steps) in interesting temperature range (figure 1). Interpretation of values calculated from $l_\tau = f(\tau)$ dependencies for individual isothermal steps is based on the use of equation (4).

Table 1. Sample composition in wt.%.

sample	α-Al_2O_3	AlOOH	PVA	graphite
1	99.9	-	0.1	-
2	93.8	6.1	0.1	
3	80.0	5.1	0.1	15.8
4	-	100	-	-

EXPERIMENTAL

To prepare the samples α-Al_2O_3 powder (ALUMALUX-39 SG, d_{50} = 1.09 μm), boehmite (CONDEA SB-1, $d \approx 5$ nm) and polyvinylalcohol - PVA (MW 49.000) as binder, graphite as pore forming material, as well as water were used.

Boehmite was peptized to a sol by standard method [13] and then thickened to a paste containing 26 wt.% of AlOOH for to be a binder.

Plastic paste was prepared from homogeneous mixture of raw materials (table 1) and a quantity of water. Then cylinders (length 1 - 2 cm, diameter 0.5 cm) were extruded from this paste and dried in open air. Samples Nos. 1 to 3 were calcined at temperature 1000°C for 1 hour and sample No. 4 (pure boehmite) was calcined at temperature 550°C.

The sintering kinetics was observed by dilatometer Netzsch 402E in series of isothermal measurements (using for all of them only one cylinder, SID method) running approx. 100 minutes at each temperature: 1100, 1150, 1200, 1250 and 1300°C. The constant temperature increase between isothermal holdings was 10°C/min. In addition to this, sample No. 4 (boehmite) was measured also at each isothermal holding using each time new sample. This procedure was later called as individual isothermal dilatometry (IID). Because the temperature range for sintering the sample No. 4 was lower, temperatures from the range of 950 to 1150°C were selected for its analysis. Shrinkage, temperature and time data were recorded at measurements. The phase composition was determined by powder X-ray analysis (Stoe) and the microstructure of sintered samples was observed by SEM (Tesla BS 300).

RESULTS

Typical dependencies (figures 1, 2) were obtained from measured dilatometry data: shrinkage (μm), temperature (°C) and time (s). They describe the length shrinkage as a function of time and temperature.

Beginning and end data of isothermal holdings were read from recorded temperature dependencies (temperature increase of 10°C/min, holding of approx. 100 min) and average temperatures for each isothermal holding were calculated using these data (table 2).

The length l_τ in time τ was calculated using measured shrinkage z according to equation

$$l_\tau = l_0 + z \tag{5}$$

where z was the measured shrinkage.

Table 2. Kinetic parameters (average temperature of isothermal stages t, formal beginning of isothermal sintering $\tau_{0,T}$, rate constant k_T, exponent n) for samples Nos. 1 to 3 and temperature range from 1100 to 1300°C and for the sample No. 4 and temperature range from 950 to 1150°C according to equation (4).

	t (°C)	$\tau_{0,T}$ (s)	$10^6 k_T$ (s^{-1})	n
1	1101.2	6067.0	0.44	0.410
	1151.3	10787.3	2.75	0.407
	1208.3	16909.3	10.90	0.374
	1251.2	23215.5	39.95	0.332
	1302.8	29072.3	158.26	0.328
2	1099.4	6265.5	0.07	0.263
	1149.9	11570.5	0.79	0.288
	1203.6	17463.3	9.24	0.328
	1253.2	23517.8	37.55	0.329
	1301.4	29641.8	164.09	0.326
3	1095.6	6154.8	0.16	0.408
	1151.4	10957.5	0.50	0.356
	1199.2	18158.3	1.09	0.298
	1251.7	23371.5	5.45	0.294
	1296.2	29147.9	20.99	0.279
4 (SID)	949.7	4921.6	0.01	0.208
	999.5	10384.7	0.46	0.246
	1049.8	16049.9	21.9	0.396
	1095.3	22822.2	305.7	0.559
	1149.6	-	-	-
4 (IID)	949.3	4857.9	0.05	0.230
	998.9	5399.2	0.03	0.223
	1049.5	6021.7	12.04	0.273
	1096.6	5614.5	352.5	0.509
	1149.3	6196.8	3396	0.800

Table 3. Activation energy of sintering E of studied samples.

sample	method	t (°C)	E (kJ/mol)
1	SID	1100-1300	541.1
2	SID	1100-1300	604.4
3	SID	1100-1300	596.7
4	SID	950-1150	950.1
4	IID	950-1150	856.1

Table 4. Bulk density before (BD^c) and after sintering (BD^s, at 1300° C - samples Nos. 1, 2, 3; 1150 °C - sample No. 4), increase of bulk density (Δ BD) during sintering and total porosity (Po) of samples Nos. 1 to 4 analyzed by SID method.

sample	1	2	3	4
BD^c (g/cm³)	2.47	2.29	1.93	1.66
BD^s (g/cm³)	2.79	3.11	2.37	2.27
Δ BD (%)	13.0	35.8	22.8	37.3
Po (%)	30.3	22.2	40.6	43.1

Table 5. Bulk density after sintering (BD^s), increase of bulk density (Δ BD) during sintering and total porosity (Po) of sample No. 4 analyzed by IID method. Bulk density before sintering BD^c = 1.66 g/cm³

t (°C)	950	1000	1050	1100	1150
BD^s (g/cm³)	1.69	1.85	2.09	2.44	2.77
Δ BD (%)	1,8	11,5	25.9	46.9	66.8
Po (%)	57.7	53.7	47.6	38.7	30.6

Final theoretical length l_f of cylinder was calculated using bulk density ρ_τ of cylinder on the end of a measurement and of its length l_τ in this time

$$l_f = \left(\frac{\rho_\tau}{\rho_s}\right)^{\frac{1}{3}} l_\tau \qquad (6)$$

where ρ_s = 3.995 g/cm³ was the density of α-Al_2O_3.

Ali and Sorensen's [10] method for SID data evaluation, which avoided the determination of formal beginning $\tau_{0,T}$ of isothermal sintering by introducing derivation, was considered by authors of this article as complicated. In addition, several attempts to use it did not provide expected linear dependencies. The reasons of this discrepancy were not analyzed, but it was thought that one possibility could be the different curve shapes caused by the big difference in particle sizes of used raw materials (5 nm and ≈ 1 μm compared with ≈16 mm of cited authors). Therefore experimental data were evaluated by classical method (at criterion of minimal sum of squared deviations) using equation (4). Three parameters k_T, n and $\tau_{0,T}$ were determined for each isothermal stage. The value of $\tau_{0,T}$ is in a sense of equation (4) such value of time τ, in which for a given temperature t the value of l_τ reaches the beginning length of cylinder l_0 (figure 3). Calculated values of parameters k_T, n and $\tau_{0,T}$ are given in table 2.

Correlation coefficients (0.9972 to 0.9999 for 600 experimental data) as well as the backward calculations show very good agreement of calculated values with experimental data. There is one isothermal step (1200°C) in the figure 4 of dilatometry dependence for sample No. 2 shown in figure 1. Backward calculation matches the experimental course of shrinkage excellently as it is evident from this picture.

Figures 5 and 6 show the dependencies of ln k_T vs. 1000/T for all of the samples according to the Arrhenius equation. Acquired values of apparent activation energy are given in table 3. Activation energy E ranges for the studied samples Nos. 1 to 3 approximately from 541 to 596 kJ/mol. Value of E increases by addition of boehmite paste and decreases by adding graphite. Activation energy E for boehmite sample is 856 kJ/mol (IID) and 950 kJ/mol (SID), respectively.

Dependencies of kinetic parameter n vs. temperature for samples Nos. 1 to 4 and SID method is shown in figure 7. The same dependencies for sample No. 4 and for

both methods (SID and IID) are shown in figure 8. Sample No. 4 underwent topotactic phase transformations (γ-δ-θ-α-Al_2O_3 [13]) during dilatometry measurement. Sintering was reduced by formation of the new α phase and practically stopped after transition phases disappeared. Phase transformations are illustrated in figure 9 at 1100°C and for IID method. Arrows in figure 2 mark disappearance of transition phases.

Sample microstructures after sintering by SID and IID dilatometry methods are shown in figure 10. Macroscopic properties as bulk density and porosity of materials are given in tables 4 and 5. Addition of boehmite to α-Al_2O_3 powder (sample No. 2) increased the bulk density - densification, and decreased the porosity. Joint addition of boehmite and graphite (sample No. 3) influenced these properties conversely. Sample No. 4 (boehmite) sintered markedly intensively by SID method as it did by IID one (table 5, figure 2).

DISCUSSION

SID and IID curves in figures 1 and 2 provide a general view on sintering of studied materials and are base for kinetic analysis of processes.

The addition of boehmite to the pure α-Al_2O_3 powder did not allow increasing the porosity of sintered body, but only by joint addition with a pore forming matter as the used graphite was. Mixture of α-Al_2O_3 and graphite could not be technically processed, because an organic binder (as the used PVA) burned out earlier than graphite did and in this way it damaged the integrity of material. In this case boehmite acted as high temperature binder after PVA burned.

Boehmite was studied not particularly from the material's point of view, but because of interpretation of kinetic results. Comparison of SID and IID methods (figure 2) revealed the importance of Al_2O_3 phase transformations on sintering. A sample running through five isothermal 100 minutes long treatments (SID) has more time for phase transformations compared with only one 100 minutes long treatment using IID method. As α-Al_2O_3 appeared in both methods at 1050°C, two responsible curves were identical. The SID sintering at 1100°C slowed, because the crystallization was over after 40 minutes, while the use of IID method (figure 9) yielded to the same state only after ≈ 100 minutes. The biggest difference between these methods was at 1150°C, when the sample practically didn't sinter at SID method, while in contrast at IID method it sintered in the greatest range. This result was a consequence of much faster sintering of transition Al_2O_3 phases in the studied temperature ranges than the sintering of thermodynamically stable α-Al_2O_3 phase.

Microstructure of samples No. 1 and 2 (figures 10 *a*, *b*) was very similar. Denser microstructure of sample No. 2 (figure 10 *b*) containing boehmite correlated with its larger bulk density (3.11 g/cm^3, table 4) compared with sample No. 1 (2.79 g/cm^3). As the grains of α-Al_2O_3 acted in the sample as seeds of boehmite, the process became more or less α-Al_2O_3 grain growth. This growth took place at expense of transition Al_2O_3 phases derived from boehmite. Adequate pores remained after graphite had burnt (figure 10 *c*). Graphite particle size enables thus to control the pores size. Microstructure of boehmite derived material (figures 10 *d*, *e*) was characterized by known vermicular microstructure [14], formed by monocrystal colonies [13,15] of the size 5-10 μm, which were more evident in a case of IID method (figure 10 *e*). On the other hand individual particles of colonies (0.5-1.0 μm) are larger (figure 10 *d*) and more evident at SID method then at IID one (figure 10 *e*).

Experimental points of rate constant match the linearity of Arrhenius equation ($\ln k_T$ vs. $1000/T$) very well (figure 5). Apparent activation energy is the lowest for pure α-Al_2O_3 (sample No. 1, 541.1 kJ/mol, table 3). This value is close to the published one (440 ± 40 kJ/mol [16]) for the grain boundary diffusion in pure α-Al_2O_3. Increase of apparent activation energy after addition of boehmite (604.4 kJ/mol, sample No. 2) and after joint addition of boehmite and graphite (596.7 kJ/mol, sample No. 3) corresponds to high values of pure boehmite (950.0 and 856.1 kJ/mol for SID and IID methods, respectively).

Temperature dependencies of parameter *n* (figures 7, 8) indicate different sintering mechanisms of α-Al_2O_3 powder and boehmite. Boehmite forms continuous phase in the system α-Al_2O_3 - AlOOH (sample No. 2), therefore the temperature dependence of parameter *n* has the same tendency as in the pure boehmite (figure 7). Graphite after burning obviously disintegrate boehmite phase, consequently the mechanism of sintering is similar to that of pure α-Al_2O_3 sample.

Decrease of parameter *n* with temperature for samples No. 1 and No. 3 corresponds to that reported by Wang et al. [11] who stated that until 1200°C a surface diffusion was the dominant sintering mechanism and above this temperature was a grain boundary one. Continuous decrease of parameter *n* with temperature indicates that mechanism of sintering continuously changes with increasing temperature. The sintering mechanism of boehmite derived Al_2O_3 is different. This could be caused by significantly smaller particles (≈ 5 nm) and by phase transformations of Al_2O_3. Sharp change of parameter *n* (from 0.275 to 0.509) in the temperature range 1050 - 1100°C (figure 8) at IID method correlates with alumina phase transformations in that temperature region. Transition alumina phases, which are the only present phases at 1050°C, completely transform to thermodynamically stable α-Al_2O_3 phase at 1100°C. Temperature dependence of parameter *n* is the same at the SID method, it is only shifted about 50°C lower due to mentioned reasons.

Characterization of boehmite gels sintering indicates that from viewpoint of high activation energy and also from temperature changes of kinetic parameter *n*, such nanometer system has some new features not described in literature. The next paper will concern these problems.

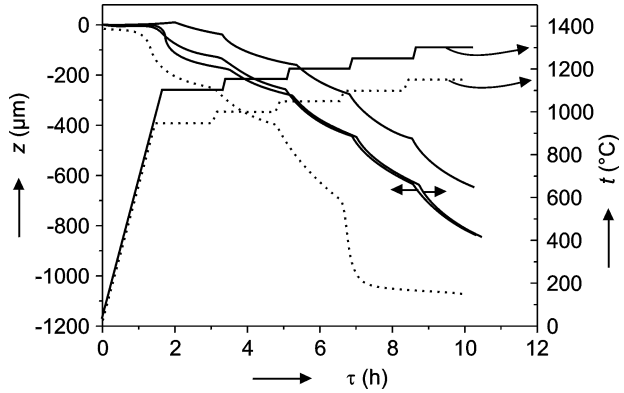

Figure 1. Normalized SID dependencies of shrinkage vs. temperature and sintering time of samples Nos. 1 to 4 (temperature increase 10°C/min). Isothermal dependencies (holding time 100 minutes) of samples Nos. 1 to 3 at temperatures 1100 - 1300°C (full lines) and of sample No. 4 (boehmite) at temperatures 950 - 1150° C (dotted lines).

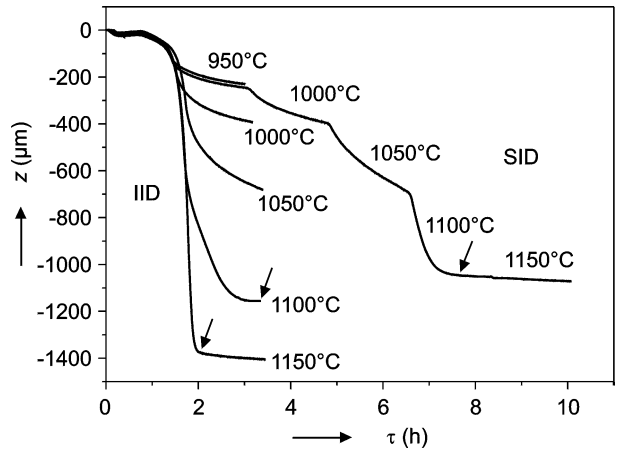

Figure 2. Comparison of SID and IID dependencies (holding time 100 min and temperature increase of 10°C/min) of sample No. 4 (boehmite).

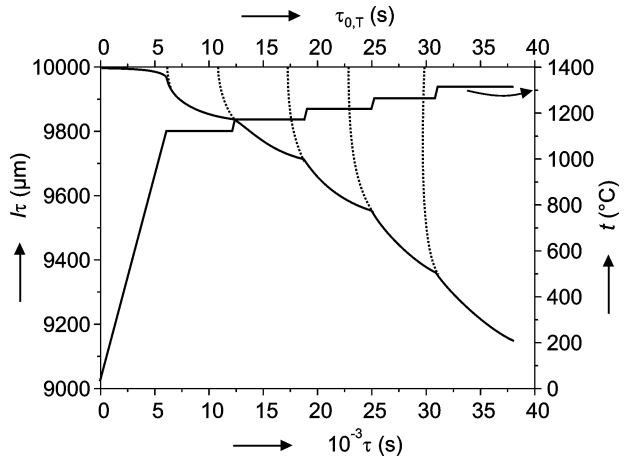

Figure 3. Values of parameter $\tau_{0,T}$ on time axis obtained from SID data (function $l_\tau = f(\tau)$) for sample No. 2.

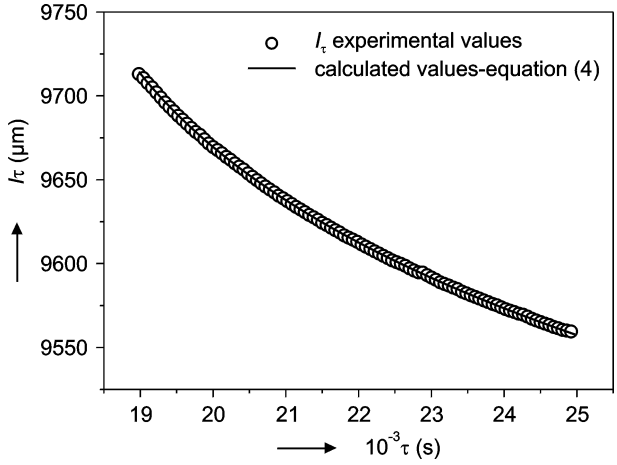

Figure 4. Comparison of experimental dependence and calculated function $l_\tau = f(\tau)$ for one isothermal measurement (1200°C, holding time 100 min) of sample No. 2 by SID method.

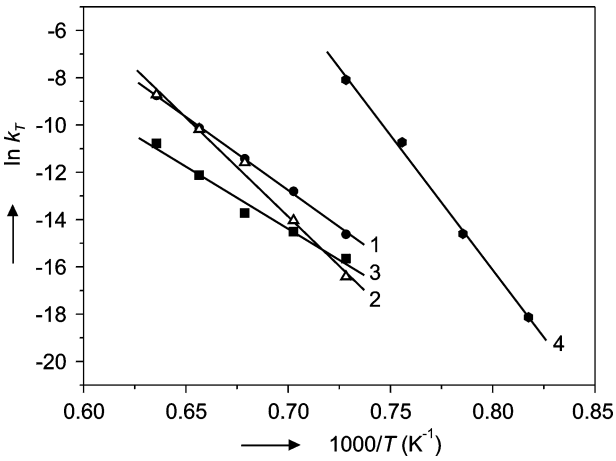

Figure 5. Plots of ln k_T vs. 1000/T of samples Nos. 1 - 4 at SID method.

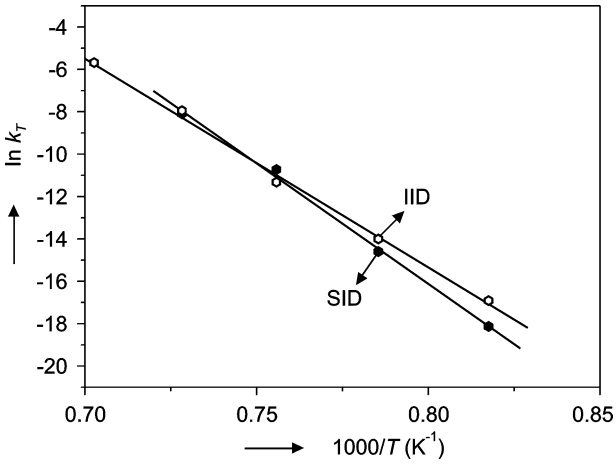

Figure 6. Plots of ln k_T vs. 1000/T of sample No. 4 at SID and IID methods.

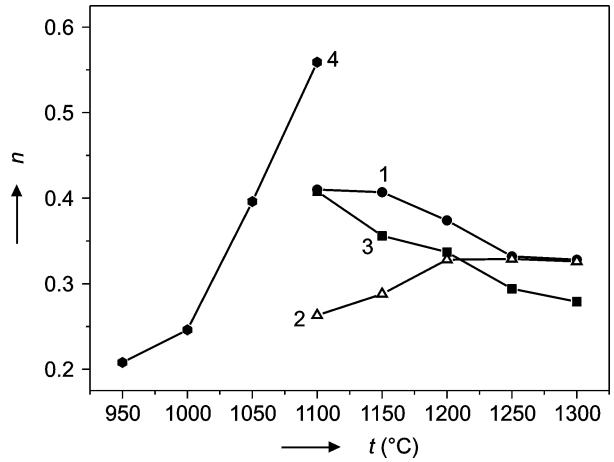

Figure 7. Plots of parameter *n* vs. temperature of all the samples at SID method.

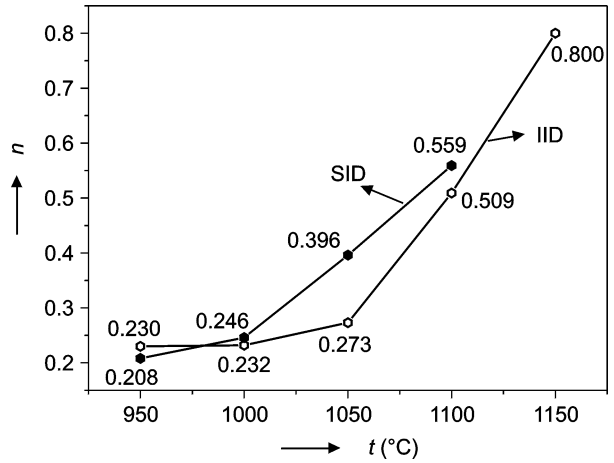

Figure 8. Plots of parameter *n* vs. temperature Sample No. 4 at SID and IID methods.

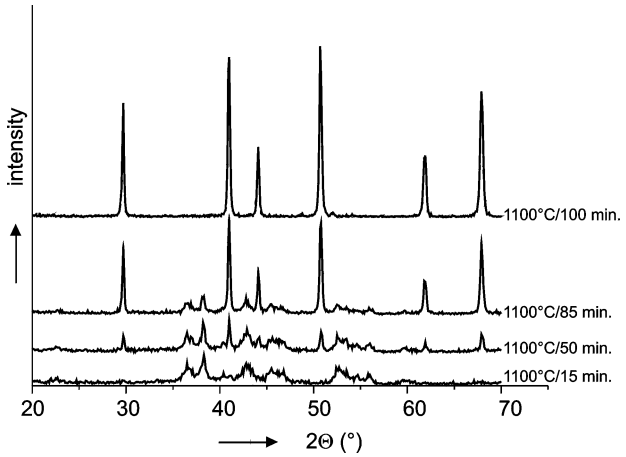

Figure 9. Phase composition of sample No. 4 (boehmite, SID method) vs. time at 1100°C.

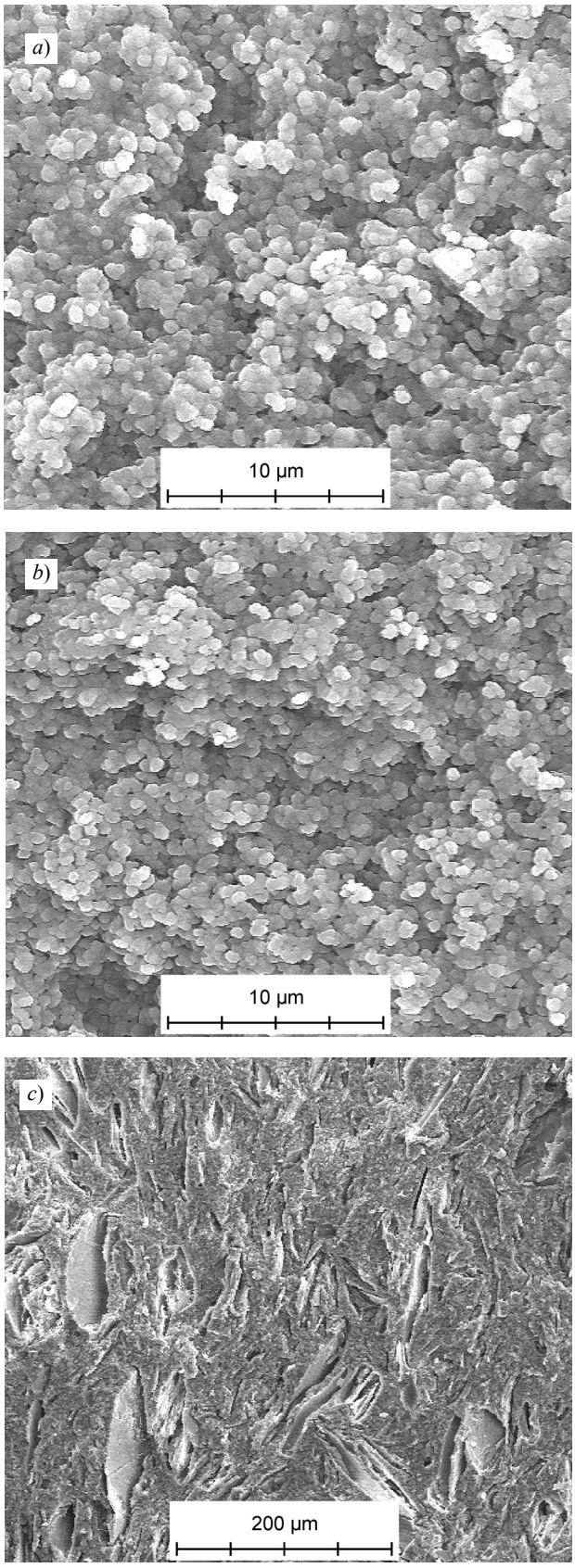

Figure 10. SEM micrograph of the sample microstructure after sintering by SID method *a*) (maximal temperature 1300 °C), No. 1, *b*) No. 2, *c*). No. 3.

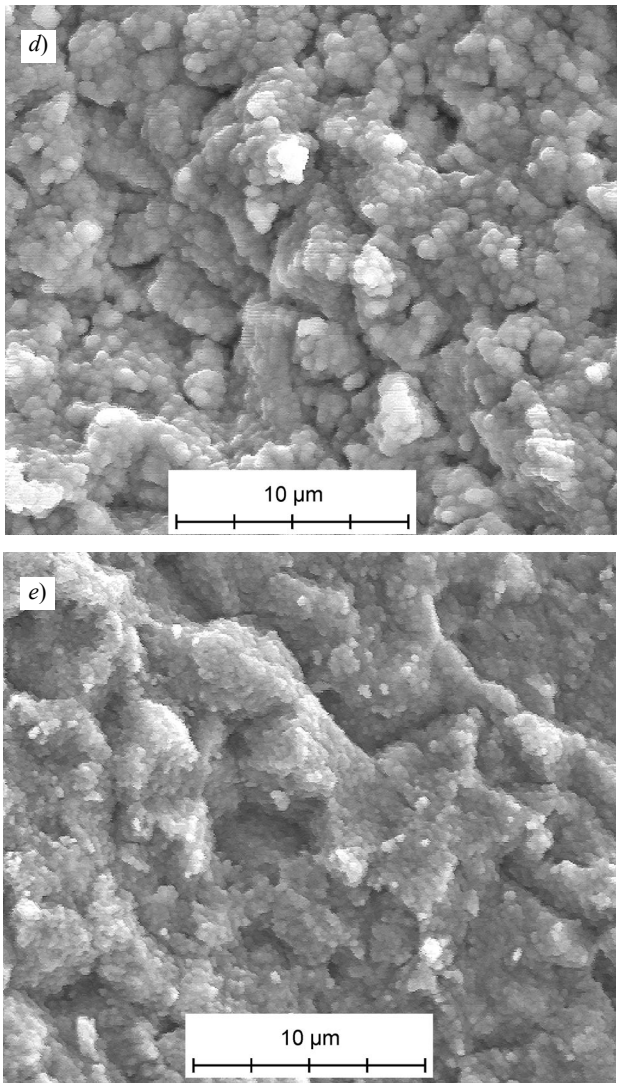

Figure 10. SEM micrograph of the sample microstructure after sintering by SID method *d*) No. 4 (maximal temperature 1150°C); sintered by IID method (1150 °C), *e*) No. 4.

CONCLUSION

SID method originally used for kinetic analysis of pressed α-Al_2O_3 powder sintering (particle size d_{50}=16.14 μm) gives good results also for significantly finer powders (1 μm and 5 nm). Evaluation of experimental data by used classical approach, however, is more favorable than that one proposed by SID method authors.

Mechanism of α-Al_2O_3 sintering continuously changes with increasing temperature (from 1100 to 1300°C) from surface to grain boundary diffusion.

Mechanism of sintering of boehmite derived alumina gels sharply changes after the transformation of transition alumina phases to α-Al_2O_3.

Porosity of α-Al_2O_3 ceramics can be effectively controlled by joint addition of boehmite paste and pore forming matter (e.g. graphite).

Acknowledgement

The Slovak Agency VEGA, Project No. 1/7353/20 and institutional project of FCHFT SUT No. 191/03, supported this research.

References

1. Keizer K., Burggraaf A. J.: Sci.Ceram. *39*, 213 (1988).
2. Trimm D.L., Stanislaus A.: Appl.Catal. *21*, 215 (1986).
3. Burggraff A. J. in: *Membrane Science and Technology Series 4*, Eds. Burggraff A. J., Cot L., Elsevier, New York 1996, p.21.
4. Gutman R. G.: *Membrane Filtration: The Technology of Pressure-driven Crossflow Processes*, Adam Hilger, Bristol 1987.
5. Matsuura T.: *Synthetic Membranes and Membrane Separation Processes*, CRC Press, Ann Arbor, 1994.
6. Riedel H., Svoboda J.: Acta Metall.Mater. *41*, 1929 (1993).
7. Kingery W. D., Bowen H. K., Uhlmann D. R.: *Introduction to Ceramics*, John Wiley & Sons, USA 1960.
8. Opfermann J., Blumm J., Emmerich W. D.: Thermochim.Acta *318*, 213 (1998).
9. Ogawa H., Kataoka Y.: High Temperature - High Pressure *13*, 481 (1981).
10. Ali M. E., Sorensen O. T., Halldahl L.: Proc. 7th Int. Conf. Thermal Analysis, Ed. B. Miller, p.344, Wiley, New York 1982.
11. Wang H., Liu X., Chen F., Meng G., Sorensen O. T.: J.Am.Ceram.Soc. *81*, 781 (1998).
12. Meng G.Y., Sorensen O.T.: Adv.Struct.Mat. *2*, 369 (1991).
13. Pach L., Roy. R., Komarneni S.: J.Mater.Res. *5*, 278 (1990).
14. Mc Ardle J.L., Messing G.L.: J.Am.Ceram.Soc. *76*, 214 (1993).
15. Pach L., Majling J., Komarneni S.: J.Sol-Gel Sci.Technol. *18*, 99 (2000).
16. Sao J.H., Harmer M.P.: Membr.Sci.Technol. *17*, 37 (1997).

DILATOMETRICKÉ SLEDOVANIE KINETIKY SPEKANIA Al_2O_3 PORÉZNEJ KERAMIKY

ZUZANA HOLKOVÁ, LADISLAV PACH, VLADIMÍR KOVÁR, ŠTEFAN SVETÍK

Fakulta chemickej a potravinárskej technológie STU, Katedra keramiky, skla a cementu, Radlinského 9, 812 37 Bratislava, Slovenská republika

Stupňovitou izotermickou a individuálnou izotermickou dilatometriou sa sledovalo spekanie extrudátov α-Al_2O_3 (zrná $d \approx 1$ μm), gélov AlOOH (častice ≈ 5 nm) a kompozícii α-Al_2O_3-AlOOH a α-Al_2O_3-AlOOH-grafit. Böhmit v kompozíciách je vysokoteplotným spojivom a grafit pórotvornou látkou. Al_2O_3 vzniknuté z böhmitu riadi spekanie sledovaných systémov ak vytvára v systéme spojitú fázu (α-Al_2O_3-AlOOH a AlOOH). Kinetické parametre (exponent-*n* a zdanlivá aktivačná energia *E*) poukazujú na rozdielny mechanizmus spekania α-Al_2O_3 a Al_2O_3 vzniknutého z böhmitového gélu. Spoločným prídavkom böhmitu a grafitu je možné riadiť porozitu α-Al_2O_3 keramiky pre účely keramických membrán.